AD

TECHNICAL REPORT ARCCB-TR-98003

TEXTURE ANALYSIS OF $CoGe_2$ ALLOY FILMS GROWN HETEROEPITAXIALLY ON GaAs(100) USING PARTIALLY IONIZED BEAM DEPOSITION

K. E. MELLO
S. L. LEE
S. P. MURARKA
T.-M. LU

19980424 135

APRIL 1998

US ARMY ARMAMENT RESEARCH, DEVELOPMENT AND ENGINEERING CENTER
CLOSE COMBAT ARMAMENTS CENTER
BENÉT LABORATORIES
WATERVLIET, N.Y. 12189-4050

APPROVED FOR PUBLIC RELEASE; DISTRIBUTION UNLIMITED

DTIC QUALITY INSPECTED 3

DISCLAIMER

The findings in this report are not to be construed as an official Department of the Army position unless so designated by other authorized documents.

The use of trade name(s) and/or manufacturer(s) does not constitute an official indorsement or approval.

DESTRUCTION NOTICE

For classified documents, follow the procedures in DoD 5200.22-M, Industrial Security Manual, Section II-19 or DoD 5200.1-R, Information Security Program Regulation, Chapter IX.

For unclassified, limited documents, destroy by any method that will prevent disclosure of contents or reconstruction of the document.

For unclassified, unlimited documents, destroy when the report is no longer needed. Do not return it to the originator.

REPORT DOCUMENTATION PAGE

Form Approved
OMB No. 0704-0188

Public reporting burden for this collection of information is estimated to average 1 hour per response, including the time for reviewing instructions, searching existing data sources, gathering and maintaining the data needed, and completing and reviewing the collection of information. Send comments regarding this burden estimate or any other aspect of this collection of information, including suggestions for reducing this burden, to Washington Headquarters Services, Directorate for Information Operations and Reports, 1215 Jefferson Davis Highway, Suite 1204, Arlington, VA 22202-4302, and to the Office of Management and Budget, Paperwork Reduction Project (0704-0188), Washington, DC 20503.

1. AGENCY USE ONLY (*Leave blank*)	2. REPORT DATE	3. REPORT TYPE AND DATES COVERED
	April 1998	Final

4. TITLE AND SUBTITLE

TEXTURE ANALYSIS OF $CoGe_2$ ALLOY FILMS GROWN HETEROEPITAXIALLY ON GaAs(100) USING PARTIALLY IONIZED BEAM DEPOSITION

5. FUNDING NUMBERS

AMCMS No. 6226.24.H191.1

6. AUTHOR(S)

K.E. Mello (RPI, Troy, NY), S.L. Lee, S.P. Murarka (RPI), and T.-M. Lu (RPI)

7. PERFORMING ORGANIZATION NAME(S) AND ADDRESS(ES)

U.S. Army ARDEC
Benet Laboratories, AMSTA-AR-CCB-O
Watervliet, NY 12189-4050

8. PERFORMING ORGANIZATION REPORT NUMBER

ARCCB-TR-98003

9. SPONSORING/MONITORING AGENCY NAME(S) AND ADDRESS(ES)

U.S. Army ARDEC
Close Combat Armaments Center
Picatinny Arsenal, NJ 07806-5000

10. SPONSORING/MONITORING AGENCY REPORT NUMBER

11. SUPPLEMENTARY NOTES

Submitted to *Journal of Applied Physics*.

12a. DISTRIBUTION/AVAILABILITY STATEMENT

Approved for public release; distribution unlimited.

12b. DISTRIBUTION CODE

13. ABSTRACT (*Maximum 200 words*)

Reflection X-Ray pole figure analysis techniques were used to study the heteroepitaxial relationships of the cobalt germanide $CoGe_2$ to GaAs(100). The alloy films were grown using the partially ionized beam deposition technique, in which low energy Ge^+ ions are used to alter the heteroepitaxial orientation of the $CoGe_2$ deposits. The $CoGe_2$[001](100)‖GaAs[100](001) orientation, which has the smallest lattice mismatch, occurred for depositions performed at a substrate temperature around 280°C and with ~1200 eV Ge^+ ions. Lowering the substrate temperature or reducing the Ge^+ ion energy leads to $CoGe_2$(100) orientation domination with $CoGe_2$[100](010)‖GaAs[100](001) and $CoGe_2$[100](001)‖GaAs[100](001). Substrate temperature alone produced only the $CoGe_2$(100) orientation. For $CoGe_2$(001) films, additional energy was required from Ge^+ ions in the evaporant stream.

14. SUBJECT TERMS

$CoGe_2$, Epitaxy, Texture, Partially Ionized Beam Deposition

15. NUMBER OF PAGES

24

16. PRICE CODE

17. SECURITY CLASSIFICATION OF REPORT	18. SECURITY CLASSIFICATION OF THIS PAGE	19. SECURITY CLASSIFICATION OF ABSTRACT	20. LIMITATION OF ABSTRACT
UNCLASSIFIED	UNCLASSIFIED	UNCLASSIFIED	UL

NSN 7540-01-280-5500

Standard Form 298 (Rev. 2-89)
Prescribed by ANSI Std. Z39-18
298-102

TABLE OF CONTENTS

Page

INTRODUCTION 1

EXPERIMENT 1

RESULTS AND DISCUSSION 2

Crystal Geometry 2

2θ Diffraction 3

Alloy Texture 4

Alloy Structure in Parameter Space 6

CONCLUSIONS 6

REFERENCES 8

TABLES

1. Three distinct types of $CoGe_2$ grains 10

LIST OF ILLUSTRATIONS

1. 2θ scan of a film grown at T_s=200°C with 1200 eV Ge^+ ions 11

2. Example of a film grown with zero eV Ge^+ ions with an elevated substrate temperature during deposition of 280°C 12

3. 2θ scan showing the dominance of the $CoGe_2$(001) orientation for a deposition with T_s=280°C and energetic 1160 eV Ge^+ ions 13

4. Surface plot of the $CoGe_2$(202) stereogram for a film grown at T_s=200°C with 1200 eV Ge^+ ions 14

5. GaAs(220) poles 15

6. $CoGe_2$(202) stereogram for a film grown with a zero accelerating potential for the Ge^+ ions and T_s=280°C 16

7. $CoGe_2$(111) stereogram for a film grown with a zero accelerating potential for the Ge^+ ions and T_s=280°C 17

Page

8. $CoGe_2$(111) poles for a sample grown with 1160 eV Ge^+ ions at T_s=280°C..................18

9. GaAs(111) poles at 54.7° with fourfold symmetry..19

10. $CoGe_2$(202) stereogram for a film grown with intermediate Ge^+ ion energies of 875 eV and T_s=280°C..20

11. Summary of the 2θ scans that show the $CoGe_2$(001) orientation formation dependence on the Ge^+ ion energy for a deposition substrate temperature of 280°C.....21

ACKNOWLEDGEMENTS

This research was supported by the National Science Foundation, Grant Number NSF ECSB9310613.

INTRODUCTION

The metallization of *n*-GaAs is a challenging engineering problem that hampers the progress of GaAs-based electronic and optoelectronic devices and circuits. Ohmic contact formation is typically achieved by alloying the GaAs with a Au-Ge film via heating to 356°C—the Au-Ge eutectic temperature. From 2-11 wt% Ni is often added to improve wetting and further reduce the barrier height (ref 1). Although many schemes for GaAs contact metallization have been developed (refs 2-11), most require alloying. The alloying process introduces nonhomogeneous interface morphology—including nonuniform regions of Ohmic contact and potential spiking problems (ref 12). This leads to problems with the quality and thermal stability of the film/GaAs interface.

Our metallization strategy follows a basic principle. Because epitaxial contacts drastically reduce or eliminate grain boundaries, they can resist chemical interaction with their semiconductor substrates at elevated temperatures (ref 13). $CoGe_2$ is a high melting point (*i.e.*, 806°C) cobalt germanide phase with a small [001] mismatch to GaAs. A high melting point heteroepitaxial contact is also expected to reduce the number of interfacial states, which are suspected of pinning the Fermi level at the GaAs surface (ref 14)—thereby making the barrier height virtually independent of the work function of the contacting material. We previously correlated $CoGe_2$ orientation to electrical behavior (ref 15)—showing $CoGe_2$(001) contacts to be Ohmic and $CoGe_2$(100) contacts to be rectifying.

Using low energy ion-surface interactions as an advanced engineering tool to improve the structure and properties of thin films has been increasingly explored in the recent literature (refs 16-18). For microelectronic applications, deriving the ions from the source material is the preferred method because self-ions do not contaminate the film. Ions in the evaporant stream increase surface mobility, provide additional energy to the growth front, sputter away light impurities (refs 19-21), and control nucleation characteristics (ref 17). The partially ionized beam (PIB) deposition method has grown high-quality epitaxial metal films (refs 22-24) and has recently produced more complicated structures, such as an epitaxial compound semiconductor and an epitaxial metallic alloy (refs 15-17). During this experiment, we studied the structural characteristics of heteroepitaxial $CoGe_2$ alloys deposited on GaAs(100) using the PIB deposition technique.

EXPERIMENT

The PIB deposition system was used to deposit the alloy films on GaAs(100) semi-insulating substrates. The PIB system is equipped with a graphite crucible surrounded by a Ta filament. Electrons are thermionically emitted from the powered Ta filament and strike the graphite crucible when high positive voltage (typically ~1200 V) is applied. A portion of the electrons travels over the mouth of the crucible and ionizes less than 2% of the exiting Ge vapor stream on impact. These ions are then accelerated by a potential applied to the substrate. The Ge^+ ions arrive at the growth front with an energy given by the potential difference between the crucible and the substrate and are deposited along with the neutral Ge species and the Co, which is conventionally evaporated in a resistively heated boron nitride (BN) crucible. The deposition

rates were selected so that the flux of the Co and Ge atoms arriving at the substrate was 1:2. Substrate preparation consisted of a 30-second wet etch in HF:H_2O 1:10, followed by drying in flowing N_2 gas. Immediately after the etch, the wafers were loaded into the chamber for deposition. A planar W heating filament was positioned approximately 3 cm above the substrate to heat the sample during deposition. The GaAs substrate was positioned under the W filament and was allowed three minutes to reach the correct temperature before the alloy deposition was started. The depositions proceeded under a vacuum of ~$5x10^{-7}$ torr, and all films were grown to a thickness of 1500 Å. The system base pressure was 10^{-7} torr. After deposition, the samples were cooled in the load lock before removal into the atmosphere.

Only two parameters were varied in this study—the Ge^+ ion energy and the deposition substrate temperature. The evaporation rates of the Co and Ge were 0.5 Å/s and 2.1 Å/s, respectively. Based on measurements of the Ge^+ ion current to the substrate holder, the percent ionization of the Ge flux is estimated to be ~1.2%. Parameter space was explored by holding the substrate deposition temperature constant and depositing a series of films—each with a different Ge^+ ion energy. The experiment was repeated at several different substrate temperatures, ranging from 100°C to 490°C. The range of Ge^+ ion energies explored varied between 0 eV and ~1400 eV. All films were grown to a thickness of 1500 Å.

After growth, the samples were characterized using a Scintag X-ray Diffraction System 2000. The phases and grain orientations in the films were analyzed using conventional 2θ X-ray diffraction. However, the 2θ scans did not adequately identify epitaxially-oriented $CoGe_2$(100) grains because their 2θ reflections coincided with the GaAs substrate peaks. A more detailed discussion of this point appears on p. 3 in the section entitled "2θ Diffraction."

A complete description of the alloy film structure was obtained using pole figure analysis (refs 25-27). To understand how this analysis worked, consider a single crystal at the center of a transparent sphere. The normal of any given plane will intersect the sphere at a point called a *pole*. When the poles on the three-dimensional surface are projected onto a two-dimensional surface while preserving the angular relationships of the planes in the actual crystal, the result is a *stereographic projection* or pole figure. In practice, the 2θ angle is fixed for Bragg diffraction of a plane of interest. The sample is then tilted incrementally in χ from 0° to 80° and rotated 360° azimuthally in ϕ about each tilt increment. The data may be plotted as a stereogram—revealing the locations of a particular family of planes with common *d* spacing. The relation between the pole locations in the stereograms from the film and substrate reveals the orientation of the film crystallites relative to the substrate.

RESULTS AND DISCUSSION

Crystal Geometry

$CoGe_2$ is orthorhombic—belonging to the C_{2v}^{17} - *Aba*2 space group, and, with a=b=5.661 Å and c=10.822 Å, the $CoGe_2$(001) orientation has only a -0.20% mismatch with GaAs(100). $CoGe_2$(100) on GaAs(100) represents an interesting situation because the $CoGe_2$ c-axis lies in the

plane of the film, and the conventional calculated lattice mismatch would be +91.5%. However, if one considers each $CoGe_2(100)$ unit cell to rest on two GaAs(100) unit cells (as viewed down the [100] direction), the mismatch is then calculated to be -4.2%. In our pole figure analysis, three distinct types of $CoGe_2$ grains formed on GaAs(100). The heteroepitaxial relationships of the three $CoGe_2$ orientations with respect to the GaAs substrates are described in Table 1.

2θ Diffraction

Information on crystallinity and phase formation was obtained by 2θ X-ray diffraction. Films deposited with a substrate temperature, T_s, during deposition of 100°C were amorphous. For films deposited at T_s=200°C, only films grown with low Ge^+ ion energies were amorphous. When a sample is grown with 1200 eV Ge^+ ions and T_s=200°C, the film crystallizes into an epitaxially-oriented $CoGe_2$ phase. The 2θ scan of this film is given in Figure 1, which shows small $CoGe_2(111)$ and $CoGe_2(222)$ peaks at 2θ angles of 23.5° and 48.3°, respectively. Peaks at 33.1° and 69.4°—which belong to $CoGe_2(004)$ and $CoGe_2(008)$—are slightly more intense. These orientations represent only a small part of the film. Most of the film consists of $CoGe_2(100)$ grains, which cannot be directly observed because of the similar interplanar spacings of $CoGe_2(200)$ with GaAs(200) and of $CoGe_2(400)$ with GaAs(400), which cause their 2θ reflections to coincide. The $CoGe_2(200)$ and $CoGe_2(400)$ peaks at 31.5° and 66.0° are *hidden* within the more powerful GaAs(200) and GaAs(400) reflections at 31.6° and 66.0°. The presence of $CoGe_2(100)$ is revealed only in the stereographic projection. The heteroepitaxial system grown at T_s=200°C with 1200 eV Ge^+ ions contains $CoGe_2$ grains with a heteroepitaxial relationship to the GaAs substrate of $CoGe_2$[100](010)||GaAs[100](001) and $CoGe_2$[100](001)||GaAs[100](001), designated as type I and type II.

A deposition substrate temperature of T_s=280°C yielded the highest degree of crystallinity for the $CoGe_2$ films (ref 15), and the balance of the study focused on the structure of films deposited at or near this temperature as a function of the Ge^+ ion energy. In all cases, $CoGe_2$ was the only phase observed. However, the orientation of the $CoGe_2$ grains relative to the substrate was found to be a function of the Ge^+ ion energy used during deposition. Films deposited at T_s=280°C that have a zero accelerating potential for the Ge^+ ions also resulted in $CoGe_2$ type I and type II structures; a 2θ scan of such a sample is presented in Figure 2. This scan reveals the $CoGe_2(004)$ and $CoGe_2(008)$ peaks—along with the substrate peaks that contain the $CoGe_2(100)$ intensity contributions. The 2θ plot does not reveal the $CoGe_2(100)$ dominating nature of the film.

When the Ge^+ ion energy is increased to 1160 eV and the deposition substrate temperature is maintained at 280°C, the $CoGe_2(001)$ orientation dominates. A 2θ plot of such a film is shown in Figure 3. The $CoGe_2(004)$ and $CoGe_2(008)$ peaks, which are present at 33.1° and 69.4°, respectively, are extremely intense and sharp. Although the $CoGe_2(200)$ and $CoGe_2(400)$ peaks are not observable, subsequent pole figure analysis shows that the $CoGe_2(100)$ orientation is nearly nonexistent in the structure, which was determined to be $CoGe_2$[001](100)||GaAs[100](001), the type III heteroepitaxial relationship. A defining feature of

the type III heterostructure is that the 2θ intensity ratio of $CoGe_2$(004) to GaAs(200) is always greater than unity.

Alloy Texture

Any preferred orientations present in the alloy crystals can be determined from an analysis of the stereograms of the $CoGe_2$ alloy films. The azimuthal (ϕ) angles at which the intensity peaks or *poles* occur—along with their radial tilt angle χ locations—reveal the azimuthal and tilt positions for any chosen family of planes $\{h,k,l\}$ with common *d* spacing in the crystal. The stereographic projection, being an equiangular map of the distributions of the $\{h,k,l\}$ plane normals, thus provides a complete description of the alloy crystal structure and orientation. Because the films are approximately 1500 Å thick, X-rays can penetrate the film, and texture analysis is possible for the GaAs substrate. The orientation of the film relative to the substrate and the epitaxial arrangement of the system can be determined by comparing stereograms of the film and substrate.

Type I and Type II Orientations

For the $CoGe_2$(202) pole figures, 2θ is set to 35.8°; therefore, the poles in the stereograms reveal the tilt and azimuthal angles for all $CoGe_2$(202) planes in the films. The pole figure that displays the pole positions in the equiangular Wulff net projection and the surface plot for intensity reference for a film grown at T_s=200°C with 1200 eV Ge^+ ions are shown in Figure 4. Because the angle between $CoGe_2$(100) and $CoGe_2$(202) is 27.6°, the four prominent poles at a tilt angle, χ, of 27.6° are the $CoGe_2$(202) poles from $CoGe_2$(100) grains. This shows that most of the film has a $CoGe_2$(100) orientation—even though this was not clearly obvious from the 2θ scan. Because $CoGe_2$ has only twofold symmetry about the [100] direction, the presence of four poles at χ=27.6° indicates that the $CoGe_2$(100) grains have two distinct heteroepitaxial arrangements with the GaAs lattice. To establish the heteroepitaxial relationships, we examined the GaAs(220) stereogram and surface plot in Figure 5. This stereogram reveals poles with fourfold symmetry at a tilt angle of 45°—the angle between GaAs(100) and GaAs(220). The GaAs(220) poles lie at precisely the same azimuthal angles as the $CoGe_2$(202) poles, which establishes the heteroepitaxial arrangement of the $CoGe_2$(100) type I and II grains as $CoGe_2$[100](010)||GaAs[100](001) and $CoGe_2$[100](001)||GaAs[100](001). Because the four film poles in Figure 4 have almost equal intensity, the alloy film contains equal volumes of $CoGe_2$(100) type I and II grains—showing no preference for either type. In addition, four very small intensity peaks are visible at χ=62.4°; these are the $CoGe_2$(202) reflections from $CoGe_2$(001) grains. Thus, $CoGe_2$[001](100)||GaAs[100](001) type III grains comprise only a small part of the film.

Raising T_s to 280°C and reducing the Ge^+ ion energy to 0 eV produces an alloy structure nearly identical to those films deposited at a lower T_s of 200°C but with 1200 eV Ge^+ ions. A typical $CoGe_2$(202) stereogram and surface plot for a deposition with T_s=280°C and a zero accelerating potential for the Ge^+ ions is shown in Figure 6. Note the similarity to Figure 4. As

before, the relationships are determined to be $CoGe_2$[100](010)||GaAs[100](001) and $CoGe_2$[100](001)||GaAs[100](001).

Stereograms of $CoGe_2$(111) poles are more complicated but contain the same information regarding alloy structure. The $CoGe_2$(111) stereogram and surface plot in Figure 7 is from the same film deposited at T_s=280°C with 0 eV Ge^+ ions. For the $CoGe_2$(100) grains in the $CoGe_2$(111) stereogram, eight planes in the {111} family can diffract. In the projection, there are only four poles at χ=48.5° for each type of $CoGe_2$(100) grain, because four of the {111} planes are crystallographically equivalent, for example, (111) and $(\bar{1}\bar{1}\bar{1})$. The angle between the (111) poles in the projection can be calculated to be ϕ=55.1° between (111) and $(11\bar{1})$ and ϕ=124.9° between (111) and $(\bar{1}1\bar{1})$. Any two adjacent poles from the {111} family will be azimuthally separated by one of these two angles. A $CoGe_2$(100) type I grain will produce four poles at ϕ=0°, 55°, 180°, and 235° (choosing the appropriate pole location to be ϕ=0); a $CoGe_2$(100) type II grain will produce precisely the same pattern but will be rotated 90° from the first angle. The eight poles observed in the Figure 7 stereogram appear at all of the angles predicted above. After noting that the GaAs(220) poles (Figure 5) appear at ϕ=62.5°, 152.5°, 242.5°, and 332.5°, the heteroepitaxial relationship of the type I and type II $CoGe_2$(100) grains to GaAs(100) is confirmed to be $CoGe_2$[100](010)||GaAs[100](001) and $CoGe_2$[100](001)||GaAs[100](001).

Type III Orientation

For alloy depositions performed at T_s=280°C and with ~1160 eV Ge^+ ions, $CoGe_2$(001) grains form the overwhelming majority of the film. Figure 8 shows the $CoGe_2$(111) stereogram and surface plot for a film grown at these conditions. Four (111) poles appear with fourfold symmetry at a tilt angle of 69.7°—the angle between the $CoGe_2$(001) and $CoGe_2$(111) planes. The GaAs(111) stereogram shown in Figure 9 displays poles at χ=54.7° with fourfold symmetry; these poles appear at exactly the same azimuthal (ϕ) angles as the $CoGe_2$(111) poles due to the equivalent fourfold symmetry of $CoGe_2$ and GaAs (111) planes viewed down the [001] direction. The $CoGe_2$(111) poles appear at a larger tilt angle because the $CoGe_2$ unit cell is larger than the GaAs unit cell in the [001] direction. When comparing stereograms of the film and substrate, we determined that the heteroepitaxial arrangement was type III with $CoGe_2$[001](100)||GaAs[100](001).

Co_5Ge_7 is the closest stoichiometric sister to $CoGe_2$. Fortunately, $CoGe_2$(111) stereograms can detect the presence of Co_5Ge_7 due to the near coincidence of the *d* spacing for $CoGe_2$(111) and Co_5Ge_7(200). Because of the similar *d* spacing of $CoGe_2$(004) with Co_5Ge_7(220) and $CoGe_2$(008) with Co_5Ge_7(440), the presence of Co_5Ge_7 could not be ruled out by 2θ diffraction. Because no Co_5Ge_7(200) poles were observed, no Co_5Ge_7 was detected in our films.

Mixed $CoGe_2$ Orientations

Alloy films deposited at T_s=280°C with intermediate Ge^+ ion energies (*i.e.*, between 300 and 900 eV) often result in films with nearly equal volumes of $CoGe_2$(100) and $CoGe_2$(001) type grains. One such example is presented in Figure 10, which shows the $CoGe_2$(202) stereogram and

surface plot for a film grown at T_s=280°C with 875 eV Ge^+ ions. The four poles at χ=27.6° are from $CoGe_2$(100) type I and $CoGe_2$(100) type II grains, while the four at χ=62.4° are from the $CoGe_2$(001) grains. Because all the pole intensities are large, the film contains significant volume fractions of each of the three types of $CoGe_2$ grains. A 2θ scan of a film grown at T_s=280°C with 875 eV Ge^+ ions is shown in Figure 11.

Alloy Structure in Parameter Space

Based on the observations discussed in the previous sections, we can now put forth some general statements regarding how alloy texture depends on the deposition parameters of substrate temperature and Ge^+ ion energy.

First, we will consider depositions with a zero accelerating potential for the Ge^+ ions. Incident ions with energies below approximately 1 eV usually do not affect film growth in a manner distinguishable from ordinary chemisorption (ref 18). So although charge transfer presumably occurs between the incident ions and surface atoms, depositions with 0 eV Ge^+ ions most closely approximate conventional vapor deposition.

Second, depositions at low substrate temperatures (*i.e.*, below 200°C) result in amorphous films. With a T_s of approximately 280°C during deposition, the film crystallizes into epitaxially-oriented $CoGe_2$(100) grains. All films deposited around this temperature with no accelerating potential for the Ge^+ ions result in the type I and type II structures.

Third, depositions performed at increased Ge^+ ion energies (and at a T_s of 280°C) result in the formation of epitaxial type III $CoGe_2$(001) grains and $CoGe_2$(100) type I and type II grains. For depositions where the Ge^+ ion energy equals approximately 1200 eV, the alloy is completely dominated by the type III orientation. Maintaining the Ge^+ ion energy at approximately 1200 eV but lowering the substrate temperature to 200°C results in the domination of type I and type II grains. Thus, formation of the type III $CoGe_2$[001](100)||GaAs[100](001) heterostructure is only possible within a very narrow window of parameter space—namely Ge^+ ion energies of approximately 1200 eV and a deposition substrate temperature near 280°C. Neither substrate temperature nor ion energy alone can produce the type III system, but a sufficient magnitude of each is required. Lowering T_s or sufficiently reducing the Ge^+ ion energy results in the preferential formation of $CoGe_2$(100). Clearly, the Ge^+ ions play a key role in obtaining $CoGe_2$(001).

CONCLUSIONS

X-ray pole figure analysis performed on $CoGe_2$/GaAs(100) heterostructures provided information on the alloy texture and revealed $CoGe_2$(100) phase formation information not detectable in ordinary Bragg diffraction experiments. Thus, heteroepitaxial relationships of the alloy and substrate were deduced by orientation information provided by stereograms of these two items. In terms of film quality, we observed the best epitaxy at a deposition substrate temperature of approximately 280°C. $CoGe_2$ phase formation was found to be a strong function

of the Ge^+ ion energy at this deposition temperature. While exploring the Ge^+ ion energy-substrate temperature parameter space, the type III heteroepitaxial orientation could not be accessed without the additional energy provided by Ge^+ ions in the evaporant stream. Lowering the substrate temperature or sufficiently reducing Ge^+ ion energy produces type I and type II heterostructures. High melting point heteroepitaxial alloys will further advance GaAs metallization and are made possible with practical technology provided by self ion-assisted heteroepitaxy.

REFERENCES

1. Robinson, G. Y., *Solid-State Electronics*, 18, 1975, p. 331.

2. Scofield, J., Liu, S., and Smith, S., *Materials Research Society Symposium Proceedings*, 282, 1993, p. 247.

3. Lustig, N., Murakami, M., Norcott, M., and McGann, K., *IBM RC*, 16, 1990, p. 365.

4. Murakami, M., and Price, W. H., *Applied Physics Letters,* 51, 1990, p. 129.

5. Wang, L. C., Wang, X. Z., Lau, S. S., Sands, T., Chan, W. K., and Keuch, T. F., *Applied Physics Letters,* 56, 1990, p. 2129.

6. Kawata, H. R., Oku, T., Otsuki, A., and Murakami, M., *Journal of Applied Physics*, 75, 1994, p. 2530.

7. Oku, T., Wakimoto, H., Otsuki, A., and Murakami, M., *Journal of Applied Physics*, 75, 1994, p. 2522.

8. Uchibori, C. J., Okunishi, M., Oku, T., Otsuki, A., Ono, N., and Murakami, M., *Journal of Electronic Materials*, 23, 1994, p. 983.

9. Marshall, E. D., Chen, W. X., Wu, C. S., Lau, S. S., and Keuch, T. F., *Applied Physics Letters*, 47, 1985, p. 298.

10. Shenoy, K. V., Fonstad, C. G., and Mikkelson, J. M., *IEEE Trans. Electron Devices*, 15, 1994, p. 106.

11. Takata, H. J., Tanakashi, K., Otsuki, A., Inui, H., and Murakami, M., *Journal of Applied Physics*, 72, 1992, p. 4191.

12. Skrabka, T., *Solid-State Electronics*, 37, 1994, p. 195.

13. Murarka, S. P., *Metallization: Theory and Practice for VLSI and ULSI,* Butterworth Heinemann, Boston, MA, 1993, p. 11.

14. Palmstrφm, C. J., and Morgan, D. V., *Gallium Arsenide: Materials, Devices, and Circuits*, John Wiley & Sons, Ltd., New York, 1985, p. 197.

15. Mello, K. E., Soss, S. R., Murarka, S. P., Lee, S. L., and Lu, T.-M., *Applied Physics Letters*, 68, 1996, p. 1817.

16. Kononenko, O. V., Matveev, V. N., Kasumov, A. Yu, Kislov, N. A., and Khodos, I. I., *Vacuum*, 46, 1995, p. 685.

17. Yun, S. J., Yoo, M. C., and Kim, K., *Journal of Applied Physics*, 74, 1993, p. 2866.

18. Atwater, H. A., *Solid State Phenomena*, 27, 1992, p. 67.

19. Yang, G.-R., Bai, P., Lu, T.-M., and Lau, W. M., *Journal of Applied Physics*, 66, 1989, p. 4519.

20. Yapsir, A. S., Lanford, W. A., and Lu, T.-M., *Applied Physics Letters*, 52, 1988, p. 1962.

21. Yang, G.-R., Bai, P., Luo, L., and Lu, T.-M., *Applied Physics Letters*, 29, 1989, p. 4519.

22. Choi, C.-H., Harper, R. A., Yapsir, A. S., and Lu, T.-M., *Applied Physics Letters*, 51, 1987, p. 1992.

23. Bai, P., Yang, G.-R., You, L., and Lu, T.-M., *Journal of Materials Research,* 5, 1990, p. 989.

24. Nason, T. C., You, L., Yang, G.-R., and Lu, T.-M., *Applied Physics Letters*, 69, 1991, p. 773.

25. Cullity, B. D., *Elements of X-ray Diffraction, 2nd Edition*, Addison-Wesley Publishing Company, Inc., Reading, MA, 1978, p. 297.

26. Wahlstrom, E. E., *Optical Crystallography, 5th Edition,* John Wiley & Sons, Ltd., New York, 1979, p. 11ff.

27. Barrett, C. S. and Massalski, T. B., *Structure of Metals, 3rd Revised Edition,* Pergamon, Oxford, 1980, Chapters 2 and 9.

Table 1. Three Distinct Types of $CoGe_2$ Grains

The grains grew heteroepitaxially on GaAs(100) substrates—depending on the substrate temperature during deposition and the Ge^+ ion energy. The heteroepitaxial relationships were determined using pole figure analysis.

Designation	$CoGe_2$ GaAs
Type I	[100](010)‖[100](001)
Type II	[100](001)‖[100](001)
Type III	[001](100)‖[100](001)

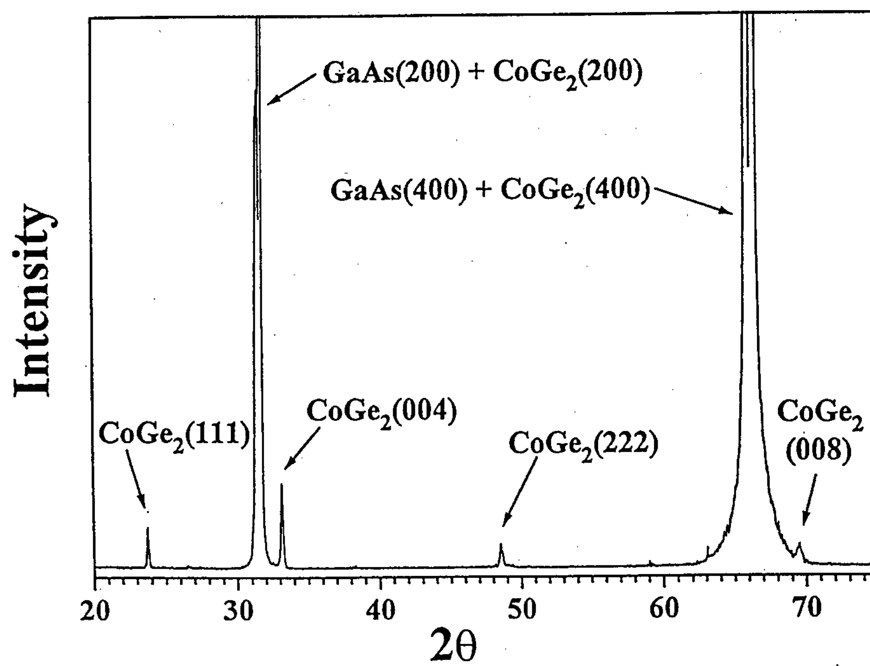

Figure 1. 2θ scan of a film grown at $T_s = 200°C$ with 1200 eV Ge^+ ions.

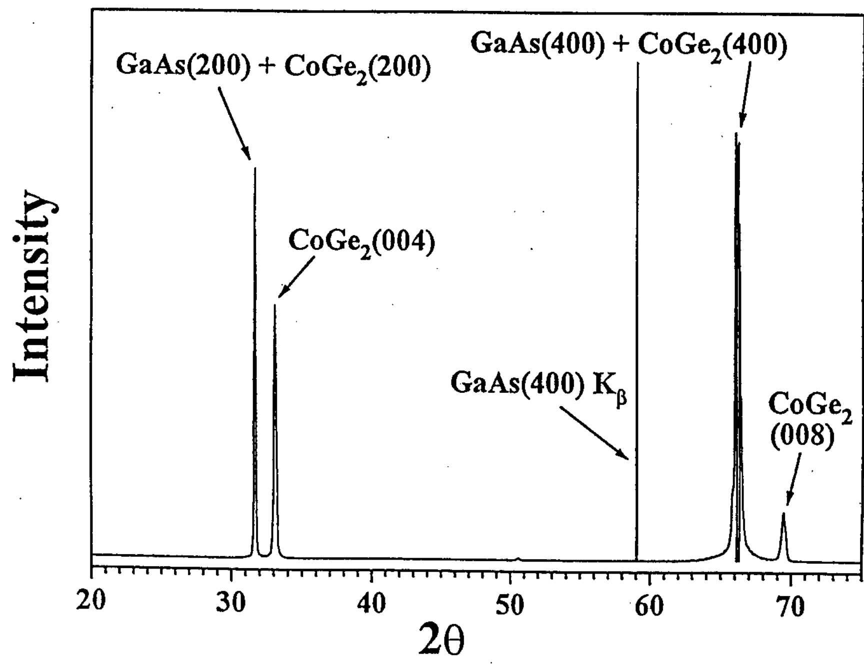

Figure 2. Example of a film grown with zero eV Ge^+ ions with an elevated substrate temperature during deposition of 280°C.

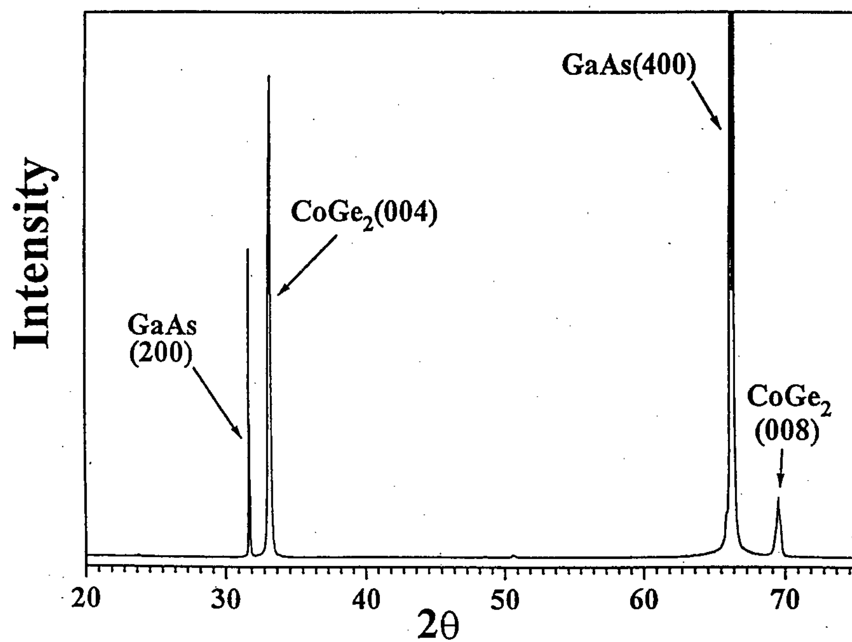

Figure 3. 2θ scan showing the dominance of the $CoGe_2(001)$ orientation for a deposition with $T_s = 280°C$ and energetic 1160 eV Ge^+ ions.

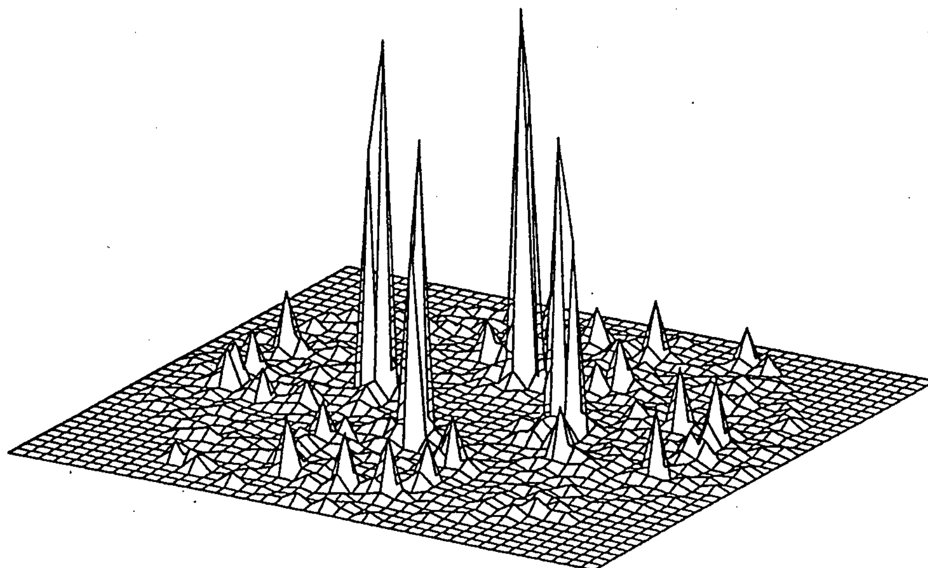

Figure 4. Surface plot of the $CoGe_2(202)$ stereogram for a film grown at $T_s = 200°C$ with 1200 eV Ge^+ ions.

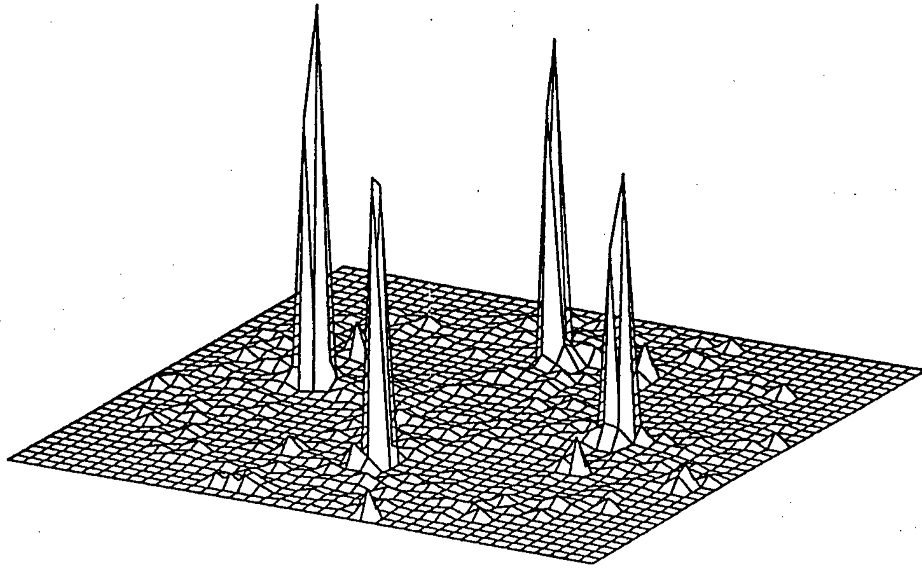

Figure 5. GaAs(220) poles.

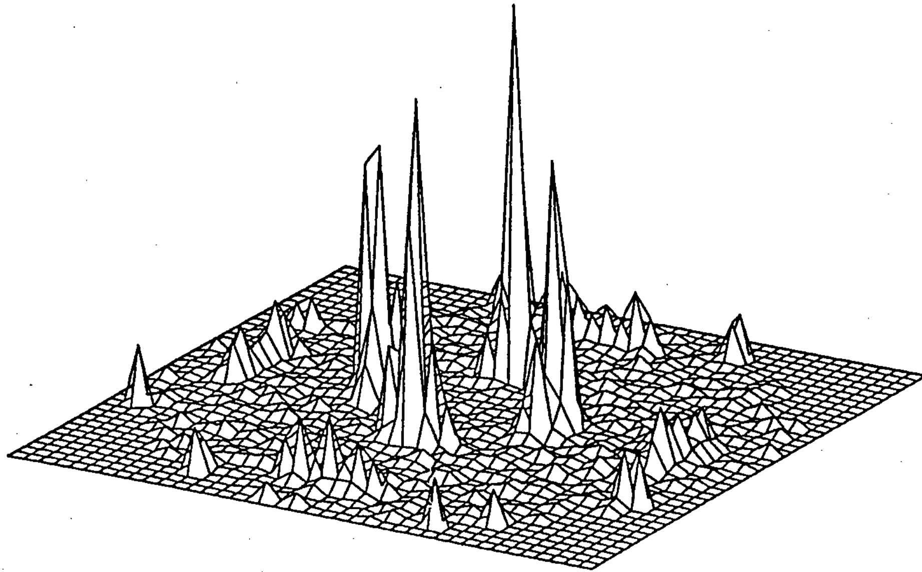

Figure 6. $CoGe_2(202)$ stereogram for a film grown with a zero accelerating potential for the Ge^+ ions and $T_s = 280°C$.

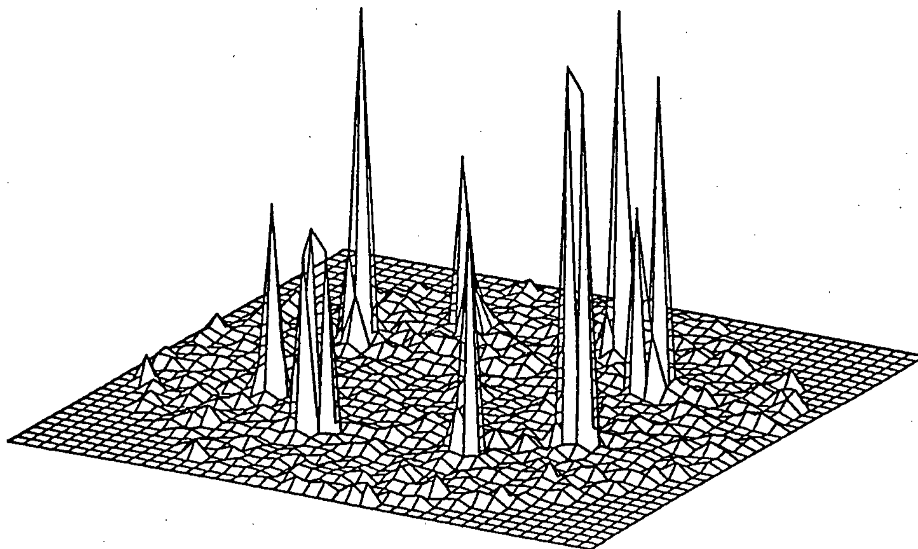

Figure 7. $CoGe_2(111)$ stereogram for a film grown with a zero accelerating potential for the Ge^+ ions and $T_s = 280°C$.

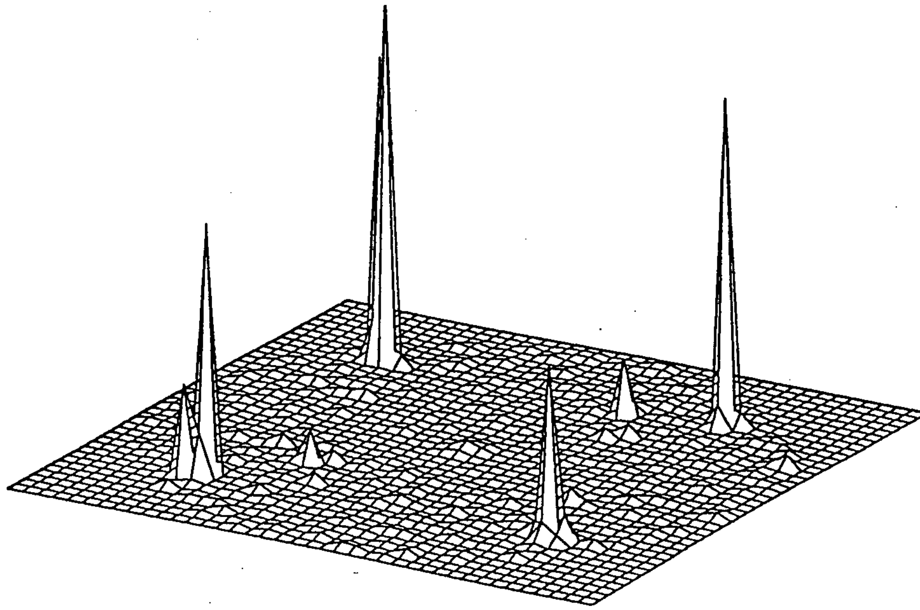

Figure 8. $CoGe_2(111)$ poles for a sample grown with 1160 eV Ge^+ ions at $T_s = 280°C$.

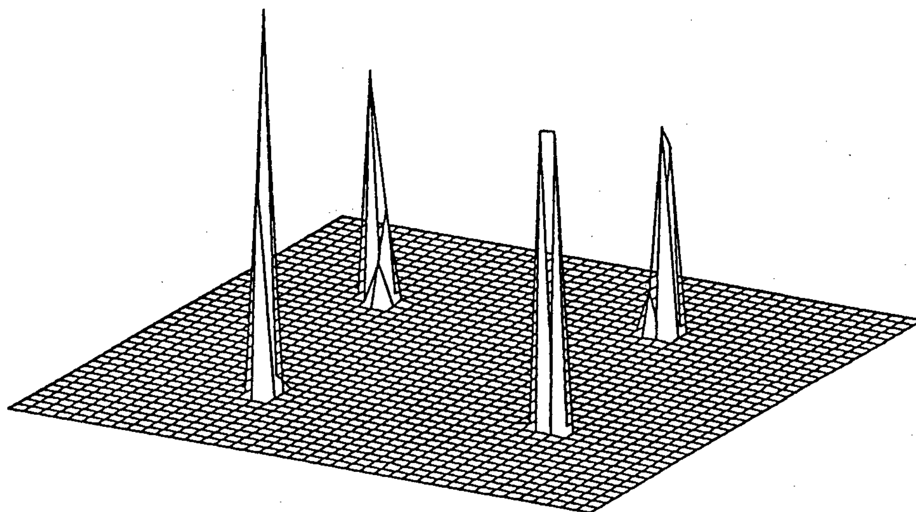

Figure 9. GaAs(111) poles at 54.7° with fourfold symmetry.

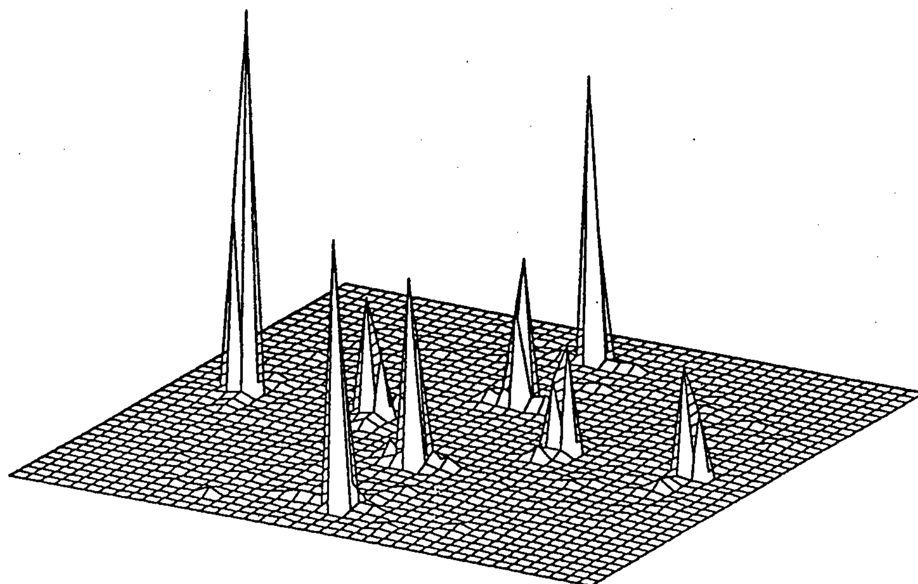

Figure 10. $CoGe_2(202)$ stereogram for a film grown with intermediate Ge^+ ion energies of 875 eV and $T_s = 280°C$.

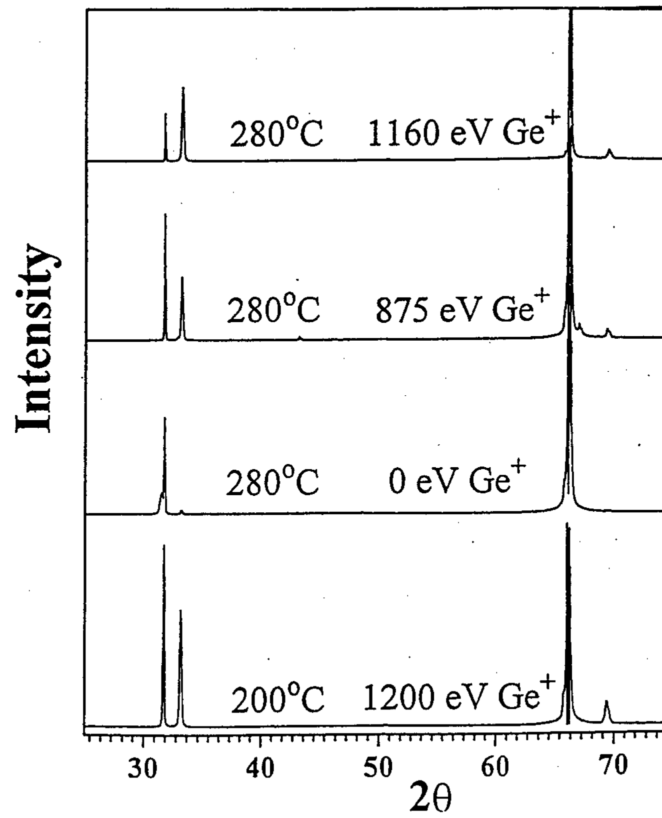

Figure 11. Summary of the 2θ scans that show the $CoGe_2$(001) orientation formation dependence on the Ge^+ ion energy for a deposition substrate temperature of 280°C.

TECHNICAL REPORT INTERNAL DISTRIBUTION LIST

	NO. OF COPIES
CHIEF, DEVELOPMENT ENGINEERING DIVISION	
ATTN: AMSTA-AR-CCB-DA	1
-DB	1
-DC	1
-DD	1
-DE	1
CHIEF, ENGINEERING DIVISION	
ATTN: AMSTA-AR-CCB-E	1
-EA	1
-EB	1
-EC	1
CHIEF, TECHNOLOGY DIVISION	
ATTN: AMSTA-AR-CCB-T	2
-TA	1
-TB	1
-TC	1
TECHNICAL LIBRARY	
ATTN: AMSTA-AR-CCB-O	5
TECHNICAL PUBLICATIONS & EDITING SECTION	
ATTN: AMSTA-AR-CCB-O	3
OPERATIONS DIRECTORATE	
ATTN: SIOWV-ODP-P	1
DIRECTOR, PROCUREMENT & CONTRACTING DIRECTORATE	
ATTN: SIOWV-PP	1
DIRECTOR, PRODUCT ASSURANCE & TEST DIRECTORATE	
ATTN: SIOWV-QA	1

NOTE: PLEASE NOTIFY DIRECTOR, BENÉT LABORATORIES, ATTN: AMSTA-AR-CCB-O OF ADDRESS CHANGES.

TECHNICAL REPORT EXTERNAL DISTRIBUTION LIST

	NO. OF COPIES
ASST SEC OF THE ARMY RESEARCH AND DEVELOPMENT ATTN: DEPT FOR SCI AND TECH THE PENTAGON WASHINGTON, D.C. 20310-0103	1
DEFENSE TECHNICAL INFO CENTER ATTN: DTIC-OCP (ACQUISITIONS) 8725 JOHN J. KINGMAN ROAD STE 0944 FT. BELVOIR, VA 22060-6218	2
COMMANDER U.S. ARMY ARDEC	
ATTN: AMSTA-AR-AEE, BLDG. 3022	1
AMSTA-AR-AES, BLDG. 321	1
AMSTA-AR-AET-O, BLDG. 183	1
AMSTA-AR-FSA, BLDG. 354	1
AMSTA-AR-FSM-E	1
AMSTA-AR-FSS-D, BLDG. 94	1
AMSTA-AR-IMC, BLDG. 59	2
PICATINNY ARSENAL, NJ 07806-5000	
DIRECTOR U.S. ARMY RESEARCH LABORATORY ATTN: AMSRL-DD-T, BLDG. 305 ABERDEEN PROVING GROUND, MD 21005-5066	1
DIRECTOR U.S. ARMY RESEARCH LABORATORY ATTN: AMSRL-WT-PD (DR. B. BURNS) ABERDEEN PROVING GROUND, MD 21005-5066	1

	NO. OF COPIES
COMMANDER ROCK ISLAND ARSENAL ATTN: SMCRI-SEM ROCK ISLAND, IL 61299-5001	1
COMMANDER U.S. ARMY TANK-AUTMV R&D COMMAND ATTN: AMSTA-DDL (TECH LIBRARY) WARREN, MI 48397-5000	1
COMMANDER U.S. MILITARY ACADEMY ATTN: DEPARTMENT OF MECHANICS WEST POINT, NY 10966-1792	1
U.S. ARMY MISSILE COMMAND REDSTONE SCIENTIFIC INFO CENTER ATTN: AMSMI-RD-CS-R/DOCUMENTS BLDG. 4484 REDSTONE ARSENAL, AL 35898-5241	2
COMMANDER U.S. ARMY FOREIGN SCI & TECH CENTER ATTN: DRXST-SD 220 7TH STREET, N.E. CHARLOTTESVILLE, VA 22901	1
COMMANDER U.S. ARMY LABCOM, ISA ATTN: SLCIS-IM-TL 2800 POWER MILL ROAD ADELPHI, MD 20783-1145	1

NOTE: PLEASE NOTIFY COMMANDER, ARMAMENT RESEARCH, DEVELOPMENT, AND ENGINEERING CENTER, BENÉT LABORATORIES, CCAC, U.S. ARMY TANK-AUTOMOTIVE AND ARMAMENTS COMMAND, AMSTA-AR-CCB-O, WATERVLIET, NY 12189-4050 OF ADDRESS CHANGES.

TECHNICAL REPORT EXTERNAL DISTRIBUTION LIST (CONT'D)

	NO. OF COPIES
COMMANDER U.S. ARMY RESEARCH OFFICE ATTN: CHIEF, IPO P.O. BOX 12211 RESEARCH TRIANGLE PARK, NC 27709-2211	1
DIRECTOR U.S. NAVAL RESEARCH LABORATORY ATTN: MATERIALS SCI & TECH DIV WASHINGTON, D.C. 20375	1
WRIGHT LABORATORY ARMAMENT DIRECTORATE ATTN: WL/MNM EGLIN AFB, FL 32542-6810	1
WRIGHT LABORATORY ARMAMENT DIRECTORATE ATTN: WL/MNMF EGLIN AFB, FL 32542-6810	1

NOTE: PLEASE NOTIFY COMMANDER, ARMAMENT RESEARCH, DEVELOPMENT, AND ENGINEERING CENTER, BENÉT LABORATORIES, CCAC, U.S. ARMY TANK-AUTOMOTIVE AND ARMAMENTS COMMAND, AMSTA-AR-CCB-O, WATERVLIET, NY 12189-4050 OF ADDRESS CHANGES.